Primary differentiated respiratory epithelial cells respond to apical measles virus infection by shedding multinucleated giant cells

Wen-Hsuan W. Lin[a,1], Annie J. Tsay[a,2], Erin N. Lalime[a,3], Andrew Pekosz[a], and Diane E. Griffin[a,4]

[a]The W. Harry Feinstone Department of Molecular Microbiology and Immunology, Johns Hopkins Bloomberg School of Public Health, Baltimore, MD 21205

Contributed by Diane E. Griffin, February 1, 2021 (sent for review June 29, 2020; reviewed by Trudy G. Morrison and Raymond J. Pickles)

Measles virus (MeV) is highly infectious by the respiratory route and remains an important cause of childhood mortality. However, the process by which MeV infection is efficiently established in the respiratory tract is controversial with suggestions that respiratory epithelial cells are not susceptible to infection from the apical mucosal surface. Therefore, it has been hypothesized that infection is initiated in lung macrophages or dendritic cells and that epithelial infection is subsequently established through the basolateral surface by infected lymphocytes. To better understand the process of respiratory tract initiation of MeV infection, primary differentiated respiratory epithelial cell cultures were established from rhesus macaque tracheal and nasal tissues. Infection of these cultures with MeV from the apical surface was more efficient than from the basolateral surface with shedding of viable MeV-producing multinucleated giant cell (MGC) syncytia from the surface. Despite presence of MGCs and infectious virus in supernatant fluids after apical infection, infected cells were not detected in the adherent epithelial sheet and transepithelial electrical resistance was maintained. After infection from the basolateral surface, epithelial damage and large clusters of MeV-positive cells were observed. Treatment with fusion inhibitory peptides showed that MeV production after apical infection was not dependent on infection of the basolateral surface. These results are consistent with the hypothesis that MeV infection is initiated by apical infection of respiratory epithelial cells with subsequent infection of lymphoid tissue and systemic spread.

primary airway cells | rhesus macaque | infected cell shedding

Measles virus (MeV) is a highly contagious enveloped, nonsegmented negative-strand RNA virus that is transmitted by the respiratory route to cause a systemic rash disease that includes pulmonary infection in both humans and nonhuman primates. Despite availability of an effective live attenuated MeV vaccine (LAMV), the worldwide incidence of measles cases and deaths has recently tripled (1, 2). Because of the efficient respiratory spread of the virus, a major hurdle for control of measles is the requirement for high vaccine-induced population immunity (92 to 95%) to interrupt transmission (3, 4).

Although the respiratory tract is the site of wild-type (WT) MeV initiation of infection and aerosol delivery of LAMV induces protective immunity (5), the biology of how MeV so efficiently initiates infection after aerosol or respiratory droplet exposure is controversial. Two fundamentally different models of MeV pathogenesis have been proposed: 1) Initial replication of MeV occurs in respiratory epithelial cells through apical infection with subsequent systemic spread to other cells and tissues; 2) Initial replication of MeV occurs in myeloid cells of the respiratory tract (alveolar macrophages/dendritic cells) with spread to other tissues and subsequent delivery by infected lymphocytes to the basolateral surface of respiratory epithelial cells for pulmonary infection and virus transmission (6, 7). The first model is supported by the presence of giant cells in broncho-alveolar lavage fluid from measles patients and identification of epithelial cell infection by histology or immunohistochemistry in the airway and lung during measles in humans and macaques (8–10). In addition, LAMV can efficiently establish pulmonary infection without producing a viremia (11), suggesting that prior infection of lymphocytes is not necessary for respiratory epithelial cell infection. The alternative model is suggested by the observation that, after pulmonary infection of macaques with recombinant MeV-expressing eGFP, the predominant $eGFP^+$ cells in the respiratory epithelium were $CD150^+$ cells and dendritic cells, not epithelial cells (12, 13). That epithelial cells are not the site of initial infection is further supported by the apparent resistance of polarized epithelial cells derived from airway tissue to infection with WT MeV via the apical surface (14, 15). Questions remain for both models.

Entry of MeV into susceptible cells is determined mainly by interaction of the hemagglutinin (H) and fusion (F) virion surface glycoproteins with receptor molecules on the host cell. The three identified cellular receptors for MeV are CD46 expressed ubiquitously in all nucleated cells (16, 17), CD150 (signaling lymphocyte activation molecule/SLAM) expressed on activated immune cells (18), and nectin-4 expressed by epithelial cells (19, 20). WT MeV can use CD150 and nectin-4 as receptors while LAMVs can utilize all three receptors. Nevertheless, in vitro and

Significance

Measles virus (MeV) is highly infectious by the respiratory route, but respiratory epithelial cells are thought to be resistant to infection through the exposed apical surface and to require infection through the basolateral surface. We show that differentiated respiratory epithelial cells are actually highly susceptible to apical infection and that infection leads to formation of multinucleated giant cells that are shed from the epithelial sheet into the lumen leaving the epithelium intact and devoid of infected cells. These results are consistent with the hypothesis that MeV infection is initiated in respiratory epithelial cells with subsequent infection of lymphoid tissue and systemic spread.

Author contributions: W.-H.W.L., E.N.L., A.P., and D.E.G. designed research; W.-H.W.L., A.J.T., and E.N.L. performed research; A.P. contributed new reagents/analytic tools; W.-H.W.L. analyzed data; and W.-H.W.L. and D.E.G. wrote the paper.

Reviewers: T.G.M., UMass Medical; and R.J.P., University of North Carolina, Chapel Hill.

The authors declare no competing interest.

[1]Present address: Department of Pathology, Columbia University, New York, NY 10032.

[2]Present address: Department of Medicine, Cambridge Health Alliance, Cambridge, MA 02139.

[3]Present address: Contamination Engineering Branch, NASA Goddard Space Flight Center, Greenbelt, MD 20771.

[4]To whom correspondence may be addressed. Email: dgriffi6@jhu.edu.

This article contains supporting information online at https://www.pnas.org/lookup/suppl/doi:10.1073/pnas.2013264118/-/DCSupplemental.

Published March 8, 2021.

in vivo spread of LAMV is more restricted than that of WT MeV (21).

The identification of nectin-4 as a functional receptor for MeV on epithelial cells (19, 20) has shed light on the pathogenesis of MeV in the respiratory tract. As an adherens junction protein, nectin-4 is located at the basolateral surfaces of epithelial cells and thus can be used by MeV to spread back into the airways after replicating systemically (22). The importance of nectin-4 in MeV transmission is highlighted by infection of macaques with a recombinant virus unable to recognize nectin-4. This nectin-4-blind virus is defective in shedding virus into the airways, although most other aspects of the infection are indistinguishable from infection caused by WT MeV (7). The observed competency of the nectin-4-blind MeV to enter and establish infection in macaques has been viewed as supporting evidence for the alternative model of MeV pathogenesis in the respiratory tract (20, 23–25). However, the mode of MeV entry into epithelial cells in vivo remains in question and the fact that nectin-4 is located on the basolateral surface of epithelial cells could also indicate that MeV enters respiratory epithelial cells from the apical surface in a nectin-4-independent manner. In particular, other modes of entry, such as endocytosis and macropinocytosis used by several paramyxoviruses, may be important for MeV entry into primary cells (26–28).

To better understand MeV infection of the respiratory tract, we have developed and characterized a primary differentiated respiratory epithelial cell culture system using tracheal and nasal epithelial cells derived from rhesus macaques (rmTEC and rmNEC), a highly relevant animal model for measles (29, 30), and compared the outcome of apical and basolateral exposure of these cells to WT MeV and LAMV. Infection occurred through both the apical surface and the basolateral surface. Apical infection was efficient and induced rapid shedding of viable MeV-infected multinucleated giant cells (MGCs) from the epithelial surface into the lumen while maintaining epithelial barrier integrity. Basal infection was less efficient with infected cells retained in the epithelial monolayer and with barrier disruption, as well as with shedding of MGCs from the apical surface.

Results

Development and Characterization of the rmTEC and rmNEC Cultures. To investigate the interaction of MeV with respiratory epithelial cells, we established primary differentiated airway epithelial cell cultures using cells derived from rhesus macaques. Methods for the growth and differentiation of these cultures were optimized for macaque cells from protocols designed for other species (31–33). In brief, epithelial cells were isolated at necropsy from the tracheas, main bronchi, and nasopharynxes of healthy macaques by digestion of tracheal, bronchial, and nasopharyngeal mucosal tissues with pronase. After fibroblast depletion, epithelial cells were expanded in growth-factor-supplemented media, frozen, and stored in liquid nitrogen. Before use, cells were thawed, expanded a second time, and plated in transwells for growth at a liquid–liquid interface. Formation of tight junctions was monitored by transepithelial electrical resistance (TEER), and, after formation (TEER of 1,000 Ω-cm^2), the predifferentiated cells were switched to an air-liquid interface (ALI) and low-nutrient media for differentiation ($\geq$14 d). Differentiated rmTEC cultures developed a pseudostratified epithelium containing ciliated, nonciliated, goblet, and basal cells with beating cilia and mucus production.

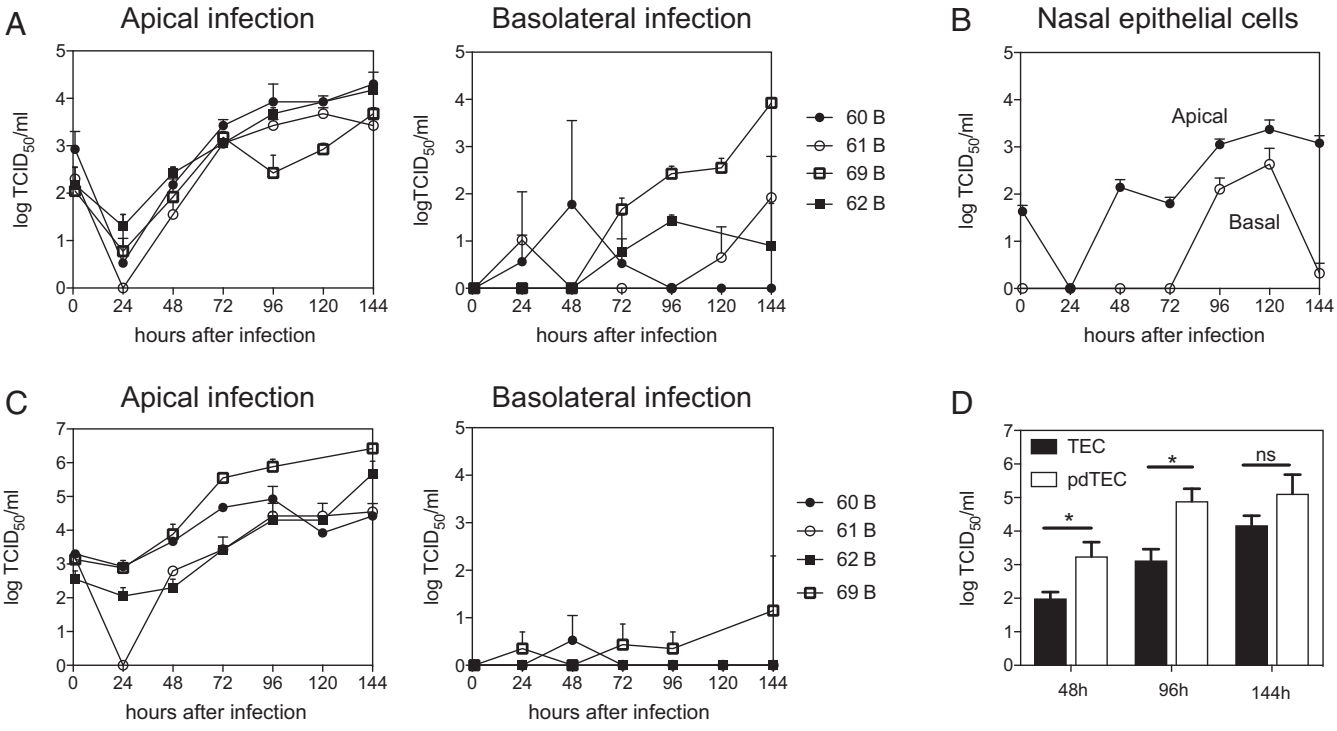

Fig. 1. Apical MeV production after apical and basolateral infection of rmTEC and rmNEC cultures with WT MeV. Cultures were infected apically and basolaterally for 4 h with WT MeV (MOI 4.5) and washed with PBS, and media was replaced. Apical and basal supernatant fluids were collected every 24 h, and $TCID_{50}$ was determined by culturing serially diluted culture fluids for 5 d on Vero/hSLAM cells. Virus was present only in apical fluids. (*A*) Apical production of infectious virus by fully differentiated rmTEC from four individual donors (60–62, 69). (*B*) Averaged amounts of infectious virus produced by fully differentiated rmNEC cultures from one donor in four experiments. (*C*) Production of infectious virus by predifferentiated rmTEC cultures from four individual donors. (*D*) Comparison of amounts of virus produced by predifferentiated (pd) and fully differentiated TEC cultures averaged from the same four donors at 48, 96, and 144 h after apical infection. Two-tailed Student's *t* tests were used for analysis. Statistical significance was determined as $*P < 0.05$.

rmTEC and rmNEC Cultures Were Permissive for WT MeV and LAMV Infection. To determine whether WT MeV can replicate in primary respiratory epithelial cell cultures, we infected (multiplicity of infection [MOI] = 4.5) fully differentiated rmTEC cells from four different donor macaques through either the apical or basolateral surface (Fig. 1*A*). After infection, fluids from the apical and basal surfaces were collected every 24 h, and infectious MeV in the fluids was assayed on Vero-hSLAM cells. Infectious MeV was present only in the apical compartment after both apical and basolateral infection with substantial variability in virus production between donors following basolateral infection (Fig. 1*A*). Similar infections with WT MeV were carried out using rmNEC cultures and also showed virus production after both apical and basolateral infection (Fig. 1*B*) although it is not known whether growth would have been enhanced at lower temperatures present in the upper respiratory tract. In both culture systems, MeV replicated more rapidly following apical infection than basolateral infection (Fig. 1 *A* and *B*). Therefore, WT MeV can infect fully differentiated rmTEC and rmNEC cultures through either the apical or basolateral surfaces but virus is released only from the apical surface.

To compare the susceptibility to infection of rmTEC cultures before and after differentiation, cultures of cells prior to ALI differentiation (predifferentiated cells) were also infected both apically and basolaterally (Fig. 1*C*). Virus production was greatest after apical infection, and predifferentiated cells produced virus more rapidly than fully differentiated cells (Fig. 1*D*), indicating that differentiation was not required for susceptibility to MeV infection.

To determine whether LAMV can replicate in macaque respiratory epithelial cell cultures, we infected fully differentiated rmTEC cells from three different donors (Fig. 2*A*) and rmNEC cells from one donor (Fig. 2*B*) with LAMV (MOI = 4.5) through either the apical or basolateral surface. Infectious MeV, assayed on Vero cells, was present in the apical compartment, but not in the basolateral compartment after both apical and basal infection. The peak titer (~10^4 $TCID_{50}$/mL) was similar between the two modes of infection in the LAMV-infected cultures (Fig. 2*A*). In general, LAMV replicated better than WT MeV in rmTEC cells after apical infection with less difference apparent for rmNEC cells (Fig. 2*C* and *SI Appendix*, Fig. S1).

Direction of MeV Entry Resulted in Distinct Cytopathic Effects. Cytopathic effects in rmTEC cultures infected apically and basolaterally with WT MeV and LAMV were characterized using phase-contrast microscopy, measurement of TEER, and immunofluorescent staining of the monolayer (Fig. 3). The detection of infectious virus in the apical compartment was common after MeV infection through either apical or basolateral surfaces (Figs. 1 and 2), but the phenotypes of the infected cells in the adherent epithelial sheet were distinct. Phase-contrast microscopy showed large syncytia in basolaterally, but not apically, infected cells (Fig. 3*A*). TEER was maintained after apical infection, but not after basolateral infection, indicating cellular damage and failure to maintain the integrity of tight junctions after basolateral infection (Fig. 3*B*). Direct immunofluorescent staining of the adherent monolayer for MeV N protein and β-tubulin showed abundant, large clusters of infected cells after basolateral MeV infection, but not after apical infection with either WT MeV or LAMV (Fig. 3*C*). Staining of MeV N protein and Zo-1, a tight-junction-associated protein, also revealed disruption of tight junctions after basolateral infection, but not after apical infection (Fig. 3*D*).

MGC Shedding Is Characteristic of MeV Infection in rmTEC Cultures. Although not present in the adherent monolayer after apical infection (Fig. 3), syncytial MGCs were present in the apical supernatant fluids (Fig. 4*A*). Multiple nuclei and high levels of viral protein were present in these giant cells consistent with MeV-induced fusion of neighboring cells to form syncytia (Fig. 4*A*). MGCs were shed into the apical supernatant fluid

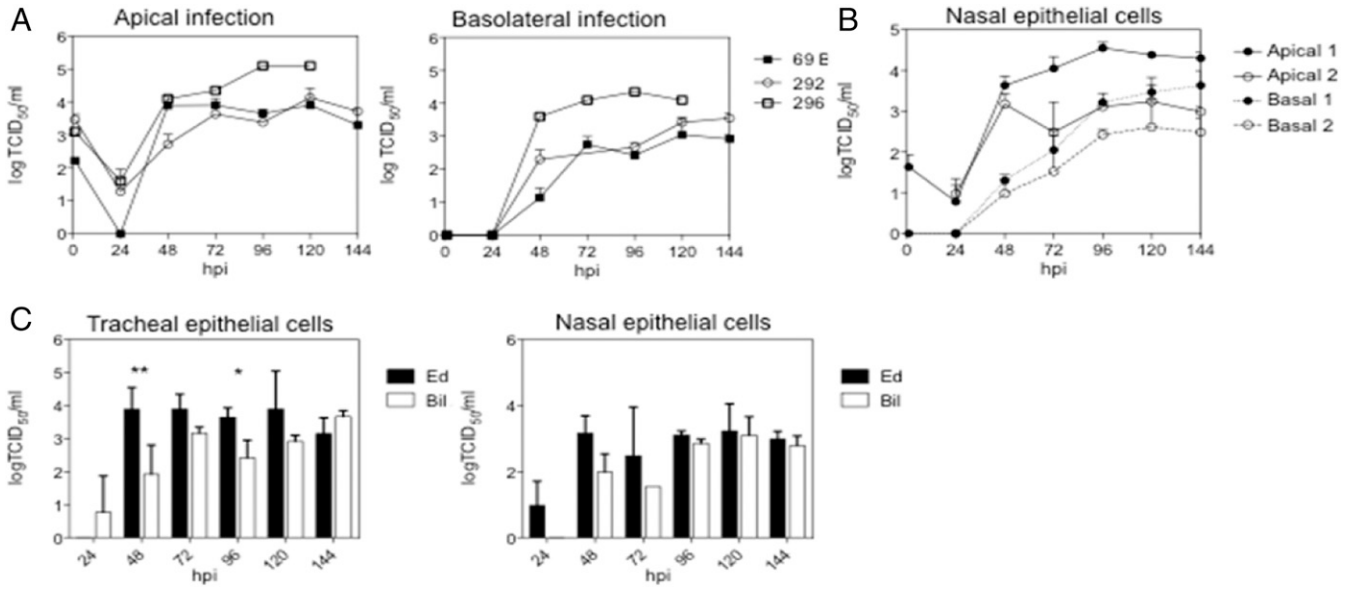

Fig. 2. Apical MeV production after apical and basolateral infection of rmTEC and rmNEC cultures with LAMV and WT MeV. Cultures were infected apically and basolaterally for 4 h with LAMV (MOI 4.5) and washed with PBS, and media was replaced. Apical and basal supernatant fluids were collected every 24 h, and $TCID_{50}$ was determined by culturing serially diluted culture fluids for 5 d on Vero (LAMV) or Vero/hSLAM (WT MeV) cells. Virus was present only in apical fluids. (*A*) Production of infectious virus by fully differentiated rmTEC from three individual donors (macaques 69, 292, 296). (*B*) Averaged amounts of infectious virus produced by fully differentiated rmNEC cultures from one donor in four experiments. (*C*) Comparison of the averaged amounts of virus produced by rmTEC and rmNEC after apical infection with WT MeV (Bil) and LAMV (Ed). Two-way ANOVAs were used for analysis. Statistical significance was indicated as $*P < 0.05$, $*P < 0.05$, $**P < 0.01$, and $***P < 0.001$. Averaged amounts of virus produced by rmTEC and rmNEC after basolateral infection with WT MeV and LAMV are shown in *SI Appendix*, Fig. S1.

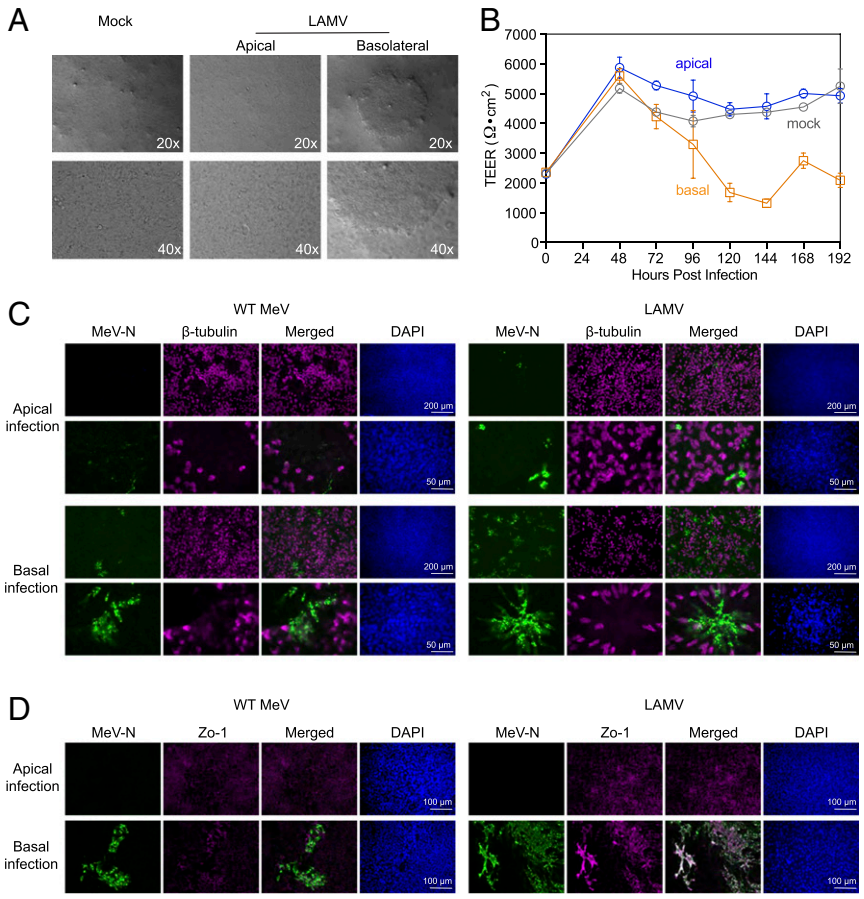

Fig. 3. Cytopathic effects and detection of viral protein in MeV-infected rmTEC cultures. rmTEC cultures were infected from either apical or basolateral surfaces for 4 h with LAMV or WT MeV (MOI = 4.5), washed with PBS and media replaced. (*A*) Phase-contrast microphotographs taken at 144 h after infection with LAMV showed large syncytia in the adherent cells after basolateral infection. (*B*) TEER monitored in rmTEC cultures that were mock-infected or infected apically or basolaterally with LAMV. (*C*) rmTEC cultures infected with WT MeV or LAMV were stained for MeV-N (green), β-tubulin (magenta), and DAPI 72 h after infection. Photomicrographs were taken at 10x (*Upper*) and 40x (*Lower*). Abundant, large syncytia were observed after basolateral MeV infection, but not following apical infection. (*D*) rmTEC cultures infected with WT MeV or LAMV were stained for MeV-N (green), Zo-1 (magenta), and DAPI. Photomicrographs were taken at 20×.

continuously for at least 6 d following apical infection with both strains of virus (Fig. 4*B*). MGC shedding into the apical supernatant fluids appears to be a common pathology after MeV infection in rmTEC cultures that occurs after apical infection as well as basolateral infection (*SI Appendix*, Fig. S2, and Movie S3).

To monitor the time course of shedding of MeV-infected cells from the apical surface, we determined the percentage of shed cells that were infected with MeV using flow cytometry and intracellular staining for MeV N protein (Fig. 5). Similar to the growth kinetics measured by the $TCID_{50}$ assay (Figs. 1 and 2), the numbers of shed MeV-infected cells increased over time and reached a peak faster following apical infection than basolateral infection (Fig. 5 *A* and *B*). To determine whether MGCs were the source of infectious MeV, we separated cells from the apical supernatant fluid by centrifugation. High titers of infectious MeV were detected in the MGCs (Fig. 5*C*), suggesting an active role for MGCs in MeV replication in the respiratory tract. Virus was also cultured from the fluid indicating release of infectious virus from the infected MGCs (Fig. 5*C*).

MGCs Were Viable and Had a Complex Subcellular Structure. Because shedding of MGCs producing infectious virus from the adherent epithelium was characteristic of MeV infection in rmTEC cultures, we further analyzed the viability and morphology of these cells (Fig. 6). Trypan blue staining (Fig. 6*A*) indicated that 60% of the cells shed into the apical supernatant fluid between 24 and 48 h after apical MeV infection were viable compared to the 20% viability of shed cells in mock-infected cultures (Fig. 6*B*). The metabolic activity of the shed cells was further analyzed with a colorless tetrazolium dye, XTT. While a majority of the shed cells from mock-infected culture remained colorless, many MGCs were able to reduce the XTT dye to brightly orange formazan, an indicator of active mitochondrial function (Fig. 6*C*). The viability of the MGCs is also evident in fused cell clusters containing actively beating cilia. Live tumbling cell clusters with beating cilia were seen in shed cells from MeV-infected cultures but not mock-infected cultures (Fig. 6*D* and Movies S1 and S2).

As MGCs appeared to play an important role in MeV infection of rmTEC cultures, we further examined the morphology of shed MGCs with transmission electron microscopy (Fig. 7). MGCs were large and possessed distinct structural features: the formation of blebs (Fig. 7 *A* and *B*) and abundant cytoplasmic vacuoles (Fig. 7 *C* and *D*). The blebs showed the same electron density as the cytoplasm, and some had a direct connection with the cell cytoplasm. The sizes of these blebs were highly variable, and many of them approximated the size of a cell (10 μm). The sizes of the cytoplasmic vacuoles were also highly variable, but

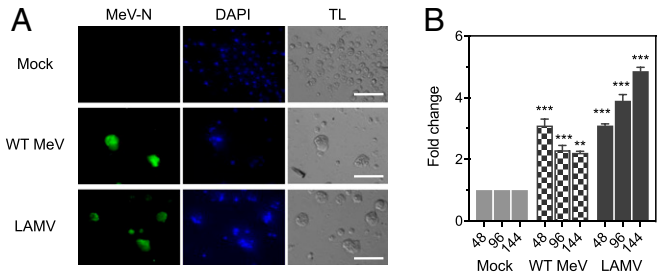

Fig. 4. MeV-infected cells shed into the apical compartment were detected by microscopy. TEC cultures were infected with WT MeV or LAMV for 4 h and washed with PBS, and media was added. Apical supernatant fluids were collected every 24 h after infection. (*A*) Cells shed to the apical supernatant fluid after apical infection with Bil-MeV, and LAMV were examined with phase-contrast microscopy or stained with antibody against MeV N after fixation and permeabilization. (Scale bar: 150 μm.) Microscopic examination of shed MGCs after basolateral infection is shown in *SI Appendix*, Fig. S2. MGCs were seen only after MeV infection but not found in mock-infected cultures. (*B*) Changes in numbers of shed cells found in rmTEC cultures from 48 to 144 h after apical infection with WT MeV (Bil) and LAMV (EZ). Shed cells were placed on slides by cytospin. Numbers of cells were quantified by counting DAPI-positive nuclei using a confocal microscope. Two-way ANOVA with Tukey's multiple comparison test comparing mock to infected at each time. $^{**}P < 0.05$, $^{***}P < 0.001$.

most had a diameter >500 nm. Many of the vacuoles were close to the cell membrane, and some were protruding or being released from the cells and resembled microvesicles, a type of releasing membrane vesicle.

Two Modes of MeV Transmission in the rmTEC Cultures. The data obtained from immunohistochemical staining and analysis of TEER (Fig. 3) suggested that different subsets of respiratory epithelial cells were infected by MeV following infection through the apical or basolateral surface. Following apical infection, the infected cells were rapidly shed, releasing MGCs into the apical compartment. Following basolateral infection, some infected cells were shed into the apical compartment, and others were resistant to shedding and formed large foci in the infected epithelial sheets. To determine whether MeV infection via different surfaces results in different modes of transmission within the rmTEC cultures, we interfered with the spread of MeV in cultures that were infected either apically or basolaterally using a fusion-inhibitory peptide (FIP) that efficiently blocks cell-to-cell fusion and spread of MeV (34) (Fig. 8). A reduction of MeV production was predicted to occur when MeV cell-to-cell spread was occurring in the compartment with FIP added. Addition of FIP to either apical or basolateral media after basolateral MeV infection reduced MeV replication (Fig. 8*B*). This indicated that both apical and basolateral spread was necessary for maintaining MeV infection following basolateral infection. However, following apical infection, reduction of MeV production occurred only when FIP was added to the apical media (Fig. 8*A*), indicating that the shed MGCs maintained production of MeV after apical infection independent of infection in the adherent epithelial cells.

Discussion

Using primary differentiated respiratory epithelial cell cultures from rhesus macaques, we show that both WT MeV and LAMV are able to infect these cells through the apical as well as the basolateral surface. Apically infected cells responded to MeV infection with syncytia formation and apical shedding of viable MGCs that exhibited blebs, cytoplasmic vacuoles, and microvesicles and were actively producing virus. Basolaterally infected cultures retained clusters of infected cells and also transmitted infection to cells for apical release (Fig. 9). After apical infection, MeV production was maintained in the rmTEC cultures through continued shedding of infected syncytial cells without detectable damage to the adherent epithelial sheet and maintenance of barrier function (Fig. 3). It is likely that apical infection was not recognized in previous studies using eGFP-expressing MeV because the infected cells are not retained in the epithelial sheet (Fig. 9). Therefore, respiratory epithelial cells were highly susceptible to apical infection and are likely target cells for initiation of infection through aerosol transmission of WT MeV, leading to systemic virus replication and spread as well as transmission of MeV infection to new susceptible hosts.

The receptor used by MeV to enter tracheal epithelial cells from the apical surface is unknown. The ability of WT MeV to infect respiratory epithelial cells in a CD150-independent manner was first observed in relevant cell lines (35, 36) and then in primary differentiated human airway cell cultures (7, 15), leading to the identification of nectin-4 as a receptor. Apical infection was equally efficient with WT MeV and LAMV (Figs. 1 and 2), consistent with the primary restriction for LAMV replication in lymphocytes rather than other primary cells (21). Neither CD150/SLAM nor nectin-4 is present on the apical surface of epithelial cells. Other modes of entry, such as endocytosis and macropinocytosis used by several paramyxoviruses, may be important for MeV entry into primary cells (26–28), and morphology of the infected cells with large membranous blebs and cytoplasmic vacuoles suggests macropinocytosis (37). Induction of macropinocytosis involves activation of actin filaments and plasma membrane ruffling that facilitates uptake of fluid and large particles and is used by several viruses for entry into epithelial cells (37–39) and facilitates nectin-4-dependent entry of MeV into colon and breast cancer cells (40).

Differentiated airway epithelial cells are susceptible to apical infection with most human respiratory viruses that have been studied, but display a variety of responses to infection (41, 42). Influenza A virus induces apoptosis in ciliated epithelial cells with extrusion of the apoptotic cells and maintenance of TEER and barrier function (43). Respiratory syncytial virus (RSV) and parainfluenza virus type 5 (PIV5) infect ciliated epithelial cells with extrusion of viable infected cells from the epithelium with rare formation of syncytia (42, 44–47). PIV3 also infects ciliated cells, but spreads within the intact epithelium without sloughing of infected cells (45, 48). In the current study, MeV infection of epithelial cells induced syncytia formation and shedding of viable MGCs from the epithelial surface while maintaining barrier function. Infection of lung organoids has also shown differential effects of respiratory virus infections. All viruses studied replicated in the organized cultures, but no morphologic changes were observed after PIV3 infection, while detachment and shedding of infected cells occurred after RSV infection and syncytia formed in response to MeV infection (45).

Thus, some viruses trigger extrusion of infected epithelial cells while others do not. Extrusion is a normal maintenance process by which epithelia simultaneously eliminate unnecessary cells and repair the gap in the epithelial sheet (49, 50). For dying cells, extrusion is induced by production of sphingosine 1 phosphate that triggers neighboring cells to activate actomyosin ring contraction to squeeze the cell out apically while bringing neighboring cells together to fill in the gap (51). Live cells in crowded epithelium are extruded through a similar process initiated by stretch-activated ion channels (52). For RSV-infected cells, extrusion is initiated during cell rounding induced by expression of the NS2 protein (47, 50). For MeV infection, it is not clear whether MGCs are induced to leave the epithelial sheet through extrusion or exfoliation, a process of accelerated turnover and shedding of superficial epithelial cells in mucosa of stratified and squamous epithelium.

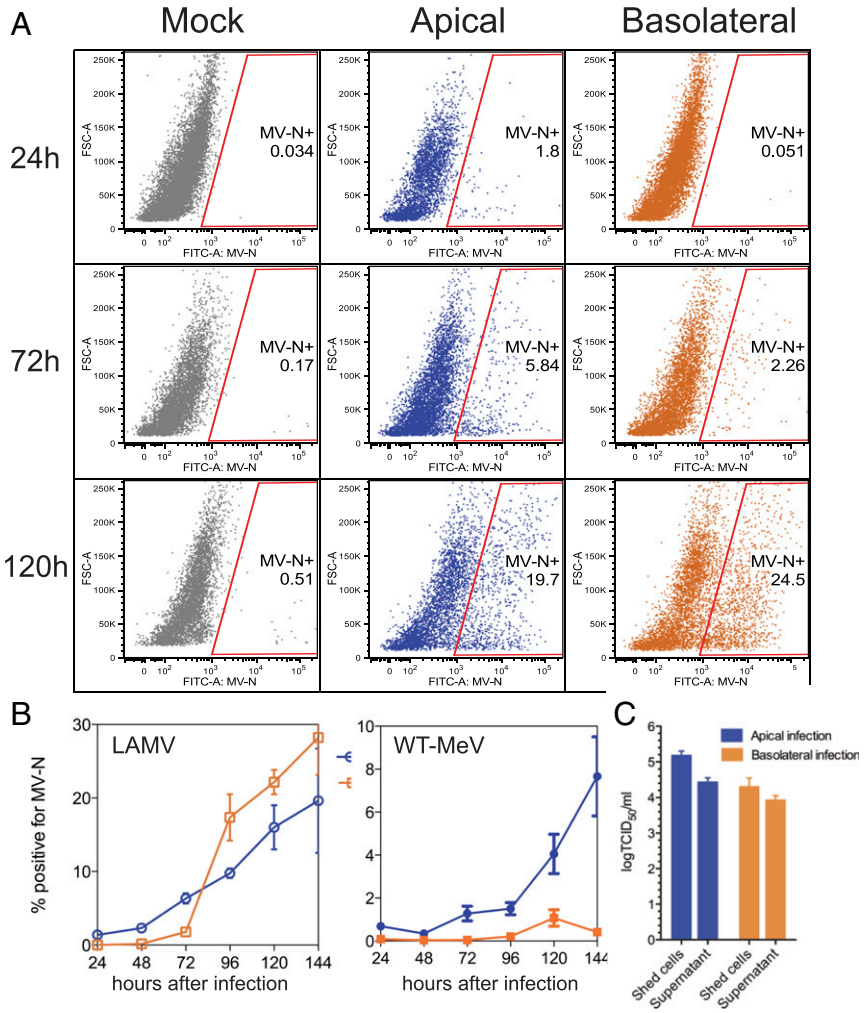

Fig. 5. MeV-infected cells shed into the apical compartment detected by flow cytometry. TEC cultures were infected with WT MeV or LAMV for 4 h and washed with PBS. (*A*) Percentage of shed cells that were LAMV-infected determined by intracellular staining for MeV-N and flow cytometry using gates generated based on mock-infected cultures at 24, 72, and 120 h. (*B*) Percentages of shed cells infected with LAMV or WT MeV after apical (blue) or basolateral (orange) infection. Graph presents results from two independent experiments with duplicates or triplicates for each experiment. (*C*) Amounts of infectious virus produced by cells and supernatant fluids of the apical compartment after apical and basolateral infection with LAMV. Cells and supernatant fluids before and after separation by centrifugation were assayed with a $TCID_{50}$ assay. Both cell-associated virus and cell-free virus were found in the apical compartment.

Exfoliation is suggested by the extensive shedding of cells induced by the interaction between MeV and the apical surface of the epithelium. Exfoliation serves as a mechanism for defending mucosal surfaces of epithelial tissues against invasion and colonization by microbes, particularly bacteria (53–56), and is triggered by signaling pathways that disrupt cell–cell and cell–matrix adhesion (57). This process often leads to caspase activation and apoptosis (termed "anoikis") (53, 55, 58), but exfoliated cells can remain viable (59) if they undergo a protective autophagic process in response to disassembly of focal adhesions and loss of matrix contact (60, 61). Further investigation is required to determine the mechanism by which viable MeV-infected MGCs are induced to leave the respiratory epithelium.

As a respiratory-transmitted systemic virus, MeV has to gain contact with $CD150^+$ lymphocytes or macrophages to access the local draining lymphoid tissue, spread systemically, and establish infection in multiple tissues (24). Although it is clear that MeV infection is initiated in the respiratory tract, it is not clear how MeV is able to cross the epithelial barrier of tightly connected pseudostratified columnar epithelial cells or the target cells for initiating infection. In contrast to the reported difficulty of infecting polarized epithelial cells with WT MeV via the apical surface (7, 15), we could consistently infect rmTEC cultures with WT MeV apically and postulate that alveolar macrophages or dendritic cells take up shed cells for transmission to the local draining lymph node (62, 63).

To understand the factors that might lead to differences in the results of our studies and those of other investigators studying the interaction of MeV with respiratory epithelial cell cultures, we compared our experimental protocol with other publications (7, 15, 35, 36). At least two differences, in addition to potential differences between differentiated cultures from humans and macaques, could influence the results. One is the readout for the MeV infection of epithelial cell cultures. Because recombinant MeV expressing eGFP is a handy tool for detecting infection without requiring cumbersome assays for infectious virus, it has been widely used for in vivo and in vitro experiments. Most studies that used MeV-eGFP for infection determined the infectivity of the virus in respiratory epithelial cell cultures by assessing the presence of green fluorescence in the adherent epithelial sheets (7, 15). However, our study has shown that infection via apical surfaces can maintain infection by rapid

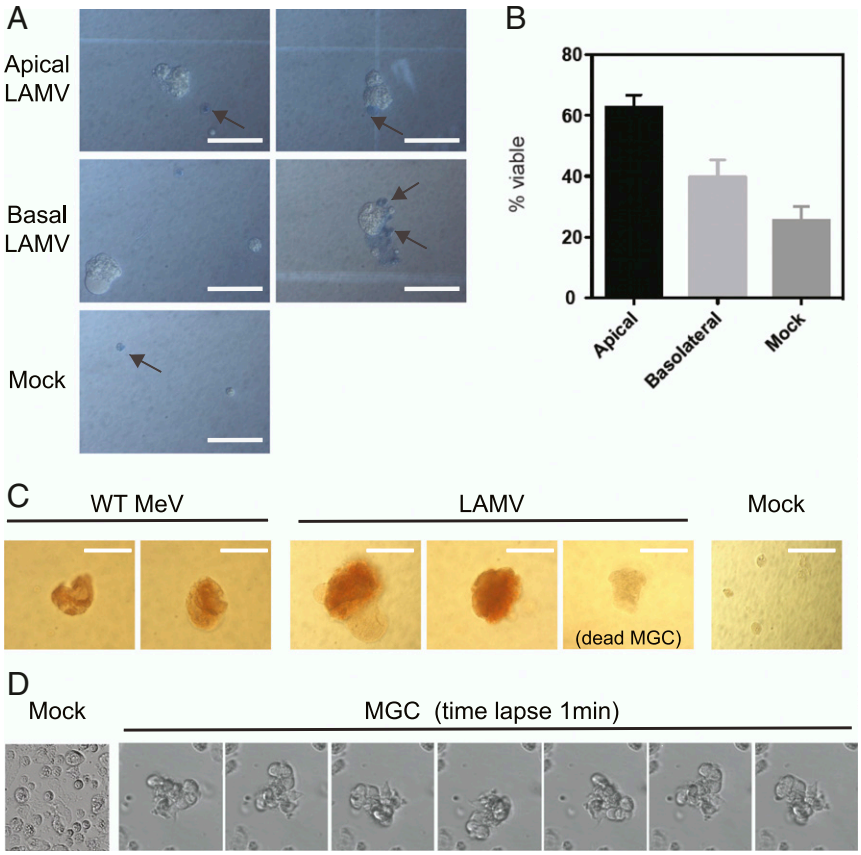

Fig. 6. Viability of the shed MGCs. (*A*) The viability of shed cells after apical and basolateral infection with LAMV was examined with trypan blue staining and light microscopy. Trypan-blue-positive dead cells are marked with arrows. (*B*) Percentages of shed cells in the apical supernatant fluid that were viable 48 h after apical or basolateral MeV or mock infection as determined by trypan blue exclusion. Graph presents results from two experiments with six replicates for each experiment. (*C*) The metabolic activity of shed cells after infection with WT MeV or LAMV was examined with a tetrazolium dye, XTT, and light microscopy. Representative images of metabolically active MGCs (orange) and dead single or multinucleated giant cells (pale or no color) from two experiments. (Scale bar: 150 μm.) (*D*) Image of shed cells from mock-infected culture and time-lapse photography over 1 min of a live tumbling MGC with beating cilia in apical supernatant fluid from a culture infected with LAMV. Corresponding time-lapse movies are in Movies S1, S2, and S3.

shedding of MGCs without causing cytopathic effects or residual infection in the adherent epithelial sheets. Therefore, a readout that focuses on the adherent epithelial sheet will miss virus that has been released or is only in the infected cells that have been shed from the apical surface. The second experimental difference is addition of medium to the apical surface after virus incubation and removal of the viral inoculum. Although cells were differentiated in ALI for 2 to 3 wk prior to MeV infection, we replaced media on the apical surfaces after washing off the MeV inoculum and replenished the apical media after collection of samples for recovery of infectious progeny virus released from the apical surface. MGCs contributed most of the infectious virus that was recovered from the apical supernatant, and MGC viability is dependent on the environment. A dry cell-free environment significantly decreases the life span of MGCs (64), so restoring apical media may have improved our detection of progeny MeV.

MGCs are the result of cell–cell fusion mediated by the interaction of viral envelope proteins H and F on the infected cell surface with cellular receptors in the plasma membranes of adjacent cells, and are a signature of MeV infection. Historically, identifying MGCs in broncho-alveolar lavage from patients was a way to diagnose measles (8, 9). In vivo, MGCs are found in the respiratory and genitourinary tract in rhesus macaques 7 d after MeV infection (10). In vitro, MeV infection of primary human small airway epithelial cells and dendritic cells induces the formation of syncytia (36, 65). In contrast, previous analysis of differentiated airway epithelial cells infected basolaterally with MeV shows efficient cell-to-cell transfer of ribonucleoprotein complexes in forming clusters of infected cells retained in the epithelial sheet (66, 67). The continuous production of MGCs following infection via the apical surface likely results from the rapid shedding of adherent cells as they become infected. The role of MGCs in supporting virus replication and regulating cell functions through formation of blebs and microvesicles has probably been underestimated (68–70). Further studies are warranted to clarify the contributions of MGC formation in the initiation of MeV infection in the respiratory tract.

Our work demonstrates that infection of respiratory epithelial cells is likely an important early step for the initiation and systemic spread of MeV. Furthermore, shedding of infected cells into the lumen of the respiratory tract may facilitate transmission of infection by respiratory secretions prior to the onset of symptoms (71). Our data are compatible with the demonstrated function of nectin-4 as a receptor for the virus to exit into the airway for transmission, as we show that MeV can infect rmTEC via the basolateral surface with apical release. Although it has been reported that most of the MeV-infected cells in the lungs of infected macaques are $CD150^+$ cells and not epithelial cells (12, 13), the tendency of MGCs to be shed from the epithelium could explain the rarity of detecting these cells in the respiratory epithelium. Moreover, because it is technically difficult to

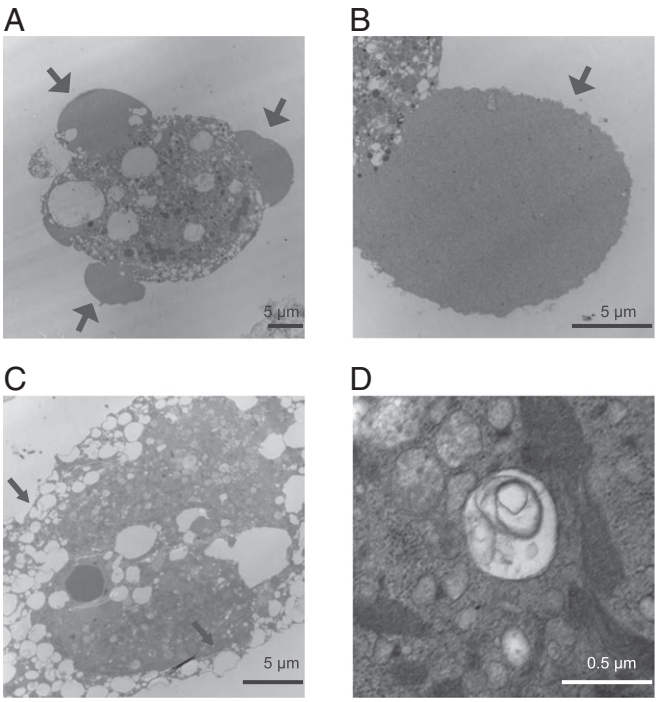

Fig. 7. Morphological characterization of MGCs at a subcellular level. Shed cells pooled from multiple wells were fixed with paraformaldehyde and analyzed by transmission electron microscopy. Two distinct structural features were found: (*A* and *B*) blebs (thick arrows) and (*C* and *D*) cytoplasmic vacuoles. Vacuoles in close proximity to the cell membrane were similar to releasing microvesicles (thinner arrows).

distinguish macrophage infection due to direct virus entry from phagocytosis of other infected cells, infection of $CD150^+$ cells in the lung may be secondary to phagocytosis of shed MGCs. As we have never observed spreading of MeV in the adherent epithelial sheets after apical infection, we think it is unlikely that the virus crosses or penetrates the epithelium to reach $CD150^+$ cells in vivo. However, it is very possible that MGCs from MeV-infected epithelial cells shed into the luminal side of the airway lead to infection of alveolar macrophages that traffic to local lymphoid tissue.

Materials and Methods

Cell Lines and Viruses. The Bilthoven strain (Bil) of WT MeV (genotype C2; a gift from Albert Osterhaus, Erasmas University, Rotterdam, Netherlands) was grown and assayed by plaque formation in Vero-hSLAM cells (72). The Edmonston-Zagreb (EZ) strain of LAMV (Serum Institute of India) was grown and assayed by plaque formation in Vero cells. Vero and Vero/hSLAM cells were grown in Dulbecco's modified Eagle's medium (DMEM) supplemented with 10% fetal bovine serum (FBS; Atlanta Biologicals).

Rhesus Macaque TEC Cultures. In brief, respiratory tracts were obtained at necropsy from two male (60, 62) and two female (61, 69) healthy rhesus macaques (*Macaca mulatta*) obtained from Harlan Laboratories after completion of a study of measles vaccination (11). All nonhuman primate studies were conducted in accordance with protocols approved by the Johns Hopkins University Animal Care and Use Committee. Tracheas were excised from below the larynx to the bifurcation of the major bronchi, cleaned, cut lengthwise, and digested for 12 to 18 h with 0.2% pronase (Sigma) in Ham's F-12 with 100 U/mL penicillin and 100 μg/mL streptomycin (Gibco) at 4 °C followed by deoxyribonuclease treatment (0.5 mg/mL in Ham's F-12) for 10 min at room temperature (RT). Cells were resuspended in TEC basic media (DMEM: F12 50:50 [Media Tech], 0.03% $NaHCO_3$, 15 mM Hepes [Gibco], 2 mM glutamine [Gibco], 250 ng/mL amphotericin B [Gibco], penicillin and streptomycin) with 10% FBS (31) and plated in a 3.5-cm cell culture plate (Falcon Primaria) for 3 h at 37 °C and 5% CO_2 to remove contaminating fibroblasts. The recovered epithelial cells were plated in a collagen-coated flask and expanded, and aliquots were frozen in liquid N_2.

Collagen-coated 0.4mm–pore 0.33 cm^2 Transwell-Clear (Corning Costar) supported membranes were used for cell growth and differentiation. Cells were plated at a density of 10^5 cells/cm^2 and grown in TEC Plus media (TEC basic with 10 μg/mL insulin, 5 μg/mL transferrin, 0.1 μg/mL cholera toxin, 25 ng/mL epidermal growth factor, 0.05 μM retinoic acid (all from Sigma), 0.03 mg/mL bovine pituitary extract [Becton Dickinson] and 5% FBS). Apical and basolateral media were changed every other day. TEER was measured with the Millipore Millicell-ERS (Millipore). Two to three days after reaching a TEER of 1,000 Ω-cm^2, the apical media was removed to create an ALI, and the basolateral media was replaced with TEC maintenance media (TEC basic with 0.05 μM retinoic acid and 2% NuSerum [Becton Dickinson]). The cells were infected between days 14 and 21 of ALI.

MeV Infection of rmTEC Cultures. ALI-rmTECs (14 to 21 d) were infected at an MOI of 4.5 with WT MeV (Bil) or LAMV (EZ). Basal media was changed a day before the infection. Stock virus was diluted in TEC maintenance media, and cells were infected through the apical surface in a total volume of 150 μL or the basolateral surface in a total volume of 500 μL for 4 h at 37 °C. The inoculum was removed and washed three times with PBS containing Ca^{2+} and Mg^{2+}. The apical or basolateral inoculum was replaced with 150 μL or 500 μL TEC maintenance media. Apical and basolateral culture fluids were collected for virus assays or fluorescence-activated cell sorting analysis at the indicated hours post infection. Infectious MeV was assayed by cocultivation

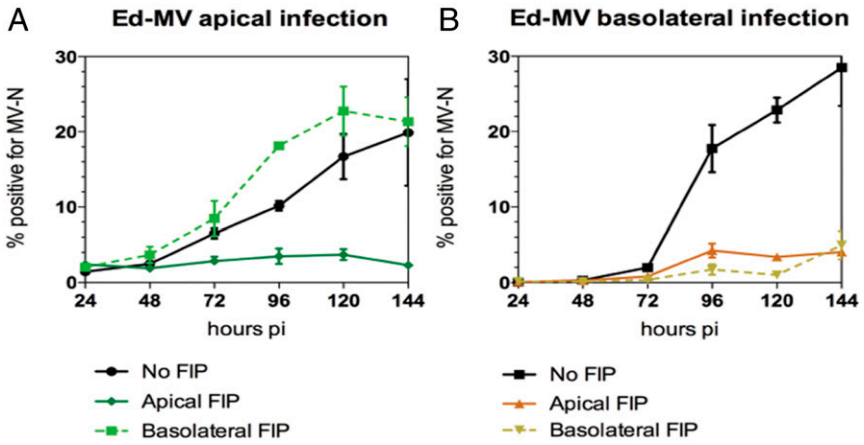

Fig. 8. Effect of blocking cell-to-cell transmission with FIP delivered apically or basolaterally on virus production. rmTEC cultures infected apically (*A*) or basolaterally (*B*) with LAMV were treated apically or basolaterally at 24 h with an FIP (80 mM) to block transmission of MeV within the culture after the first round of infection. Apical supernatant fluids were analyzed for percentage of shed cells that were MeV infected. Graph presents results from two independent experiments with duplicates or triplicates for each experiment.

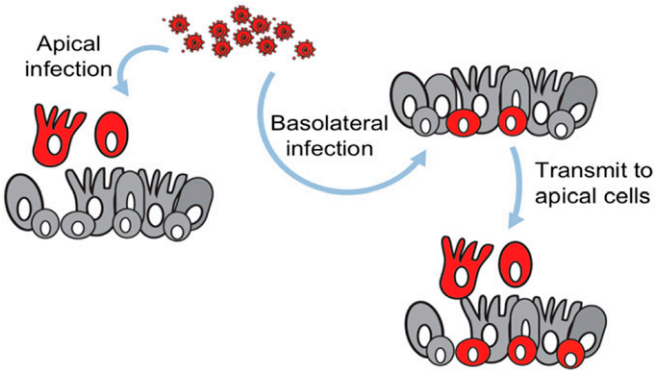

Fig. 9. Different modes MeV transmission in rmTEC cultures after apical and basolateral infection. Following apical infection, the infected cells are rapidly released into the apical compartment without infecting the basal cells. Following basolateral infection, virus spreads laterally to form large syncytia with transmission to more superficial cells that are shed into the apical compartment after infection.

of serially diluted culture fluids with Vero or Vero/hSLAM cells in four replicate wells. Cultures were scored for cytopathic effect after 5 d, and data reported as tissue culture infectious dose 50% ($TCID_{50}$) per milliliter. For experiments using fusion-inhibitory peptides (FIP, Z-D-PHE-PHE-GLY-OH, Bachem), cells were infected as above. After washing, TEC maintenance media containing 80 mM FIP replaced either the apical or the basolateral media.

Immunofluorescence Microscopy. rmTECs grown on the transwell inserts were washed with PBS and fixed in 2% paraformaldehyde for 15 min at RT. After fixation, the cells were washed with PBS and permeabilized with PBS containing 0.2% Triton X-100 for 10 min. The cells were blocked with PBS containing 3% normal goat serum and 0.5% bovine serum albumin (blocking buffer) for 30 min. The cells were then incubated with the primary antibody in blocking buffer for 1 h, washed, and incubated with secondary antibodies for 45 min. Mouse anti–β-tubulin IV (BioGenex), rabbit polyclonal anti-Zo1 (Invitrogen), and mouse anti-mucin 5AC (Muc5AC, NeoMarkers) were used to stain ciliated cells and goblet cells with AlexaFluor 555-conjugated goat anti-mouse antibody as the secondary antibody. All washes were performed with PBS containing 0.2% Tween 20. The membrane inserts were mounted with Molecular Probes Prolong antifade containing DAPI (Invitrogen) for nuclei staining. The cells were examined using a Nikon-90i confocal microscope. Images were analyzed using Volocity (Quorum Technologies) and Image J software.

Examination of Cell Morphology and Detection of MeV Antigens. Cytopathic effects of MeV infection on rmTEC cultures were examined with a Nikon inverted TE200 microscope. Shed cells from rmTEC cultures were plated on 96-well flat-bottom plates and centrifuged, and supernatant fluid was removed. For viability, trypan blue dye was added to shed cells and examined using a light microscope. For metabolic activity, activated-XTT Solution (ATCC) prepared following the manufacturer's protocol was added to shed cells, cultured at 37 °C for 2 h, and examined using a light microscope. For detection of viral antigen, shed cells were fixed and permeabilized using a BD Cytofix/Cytoperm kit, washed, and incubated with fluorescein isothiocyanate (FITC)-conjugated antibody to MeV N (Chemicon) in cytoperm wash solution for 1 h at 4 °C followed by DAPI for 15 min. The cells were examined using a Nikon inverted TE200 microscope. For quantification of the number of shed cells, cells from the apical culture fluid were spun onto slides by Cytospin. The slides were mounted with Molecular Probes Prolong antifade containing DAPI for staining nuclei, examined using a Nikon-90i confocal microscope, and counted.

To examine the subcellular structures of MeV-infected shed cells, cells were collected from rmTEC cultures. After centrifugation, cell pellets were fixed with paraformaldehyde and glutaraldehyde and sectioned. The cells were examined using a Philips/FEI BioTwin CM120 transmission electron microscope.

Flow Cytometry. Shed cells were collected from rmTEC cultures and plated on 96-well plates. Supernatant fluid was removed after centrifugation. The cells were then fixed and permeabilized using the BD Cytofix/Cytoperm kit. After washing, the cells were incubated with FITC-conjugated MeV N-specific antibody in cytoperm wash solution for 1 h at 4 °C. The cells were read on a FACSCanto II flow cytometer. Data were analyzed using FlowJo software (BD Life Sciences)

Statistical Analysis. For statistical analyses, we performed two-tailed Student's *t* test ($\alpha = 0.05$) or ANOVA with Bonferroni posttests. All data were analyzed using GraphPad Prism software. Statistical significance was determined with $*P < 0.05$, $**P < 0.01$, and $***P < 0.001$.

Data Availability. All study data are included in the article and/or supporting information.

ACKNOWLEDGMENTS. This work was funded by NIH Grants R01 AI131228, AI153140, and AI023047 (to D.E.G.); Center of Excellence in Influenza Research and Surveillance contract HHS N272201400007C (to A.P.) from the NIH; a Johns Hopkins Provost Undergraduate Research Award (to A.J.T.); and the Marjorie Gilbert Student Scholarship Fund (W.-H.W.L.).

1. A. Dabbagh *et al.*, Progress toward regional measles elimination: Worldwide, 2000–2017. *MMWR Morb. Mortal. Wkly. Rep.* **67**, 1323–1329 (2018).
2. C. I. Paules, H. D. Marston, A. S. Fauci, Measles in 2019: Going backward. *N. Engl. J. Med.* **380**, 2185–2187 (2019).
3. F. M. Guerra *et al.*, The basic reproduction number (R_0) of measles: A systematic review. *Lancet Infect. Dis.* **17**, e420–e428 (2017).
4. N. J. Gay, G. De Serres, C. P. Farrington, S. B. Redd, M. J. Papania, Assessment of the status of measles elimination from reported outbreaks: United States, 1997–1999. *J. Infect. Dis.* **189**, S36–S42 (2004).
5. D. E. Griffin, Current progress in pulmonary delivery of measles vaccine. *Expert Rev. Vaccines* **13**, 751–759 (2014).
6. M. Ludlow *et al.*, Measles virus infection of epithelial cells in the macaque upper respiratory tract is mediated by subepithelial immune cells. *J. Virol.* **87**, 4033–4042 (2013).
7. V. H. Leonard *et al.*, Measles virus blind to its epithelial cell receptor remains virulent in rhesus monkeys but cannot cross the airway epithelium and is not shed. *J. Clin. Invest.* **118**, 2448–2458 (2008).
8. R. Lightwood, R. Nolan, Epithelial giant cells in measles as an acid in diagnosis. *J. Pediatr.* **77**, 59–64 (1970).
9. M. Akhtar, I. Young, Measles giant cell pneumonia in an adult following long-term chemotherapy. *Arch. Pathol.* **96**, 145–148 (1973).
10. M. B. McChesney *et al.*, Experimental measles. I. Pathogenesis in the normal and the immunized host. *Virology* **233**, 74–84 (1997).
11. W. H. Lin *et al.*, Successful respiratory immunization with dry powder live-attenuated measles virus vaccine in rhesus macaques. *Proc. Natl. Acad. Sci. U.S.A.* **108**, 2987–2992 (2011).
12. R. L. de Swart *et al.*, Predominant infection of CD150+ lymphocytes and dendritic cells during measles virus infection of macaques. *PLoS Pathog.* **3**, e178 (2007).
13. K. Lemon *et al.*, Early target cells of measles virus after aerosol infection of nonhuman primates. *PLoS Pathog.* **7**, e1001263 (2011).
14. P. L. Sinn, G. Williams, S. Vongpunsawad, R. Cattaneo, P. B. McCray Jr, Measles virus preferentially transduces the basolateral surface of well-differentiated human airway epithelia. *J. Virol.* **76**, 2403–2409 (2002).
15. M. Ludlow *et al.*, Wild-type measles virus infection of primary epithelial cells occurs via the basolateral surface without syncytium formation or release of infectious virus. *J. Gen. Virol.* **91**, 971–979 (2010).
16. D. Naniche *et al.*, Human membrane cofactor protein (CD46) acts as a cellular receptor for measles virus. *J. Virol.* **67**, 6025–6032 (1993).
17. R. E. Dörig, A. Marcil, A. Chopra, C. D. Richardson, The human CD46 molecule is a receptor for measles virus (Edmonston strain). *Cell* **75**, 295–305 (1993).
18. H. Tatsuo, N. Ono, K. Tanaka, Y. Yanagi, SLAM (CDw150) is a cellular receptor for measles virus. *Nature* **406**, 893–897 (2000).
19. R. S. Noyce *et al.*, Tumor cell marker PVRL4 (nectin 4) is an epithelial cell receptor for measles virus. *PLoS Pathog.* **7**, e1002240 (2011).
20. M. D. Mühlebach *et al.*, Adherens junction protein nectin-4 is the epithelial receptor for measles virus. *Nature* **480**, 530–533 (2011).
21. W. W. Lin *et al.*, A durable protective immune response to wild-type measles virus infection of macaques is due to viral replication and spread in lymphoid tissues. *Sci. Transl. Med.* **12**, eaax7799 (2020).
22. V. Racaniello, Virology. An exit strategy for measles virus. *Science* **334**, 1650–1651 (2011).
23. M. Takeda, Measles virus breaks through epithelial cell barriers to achieve transmission. *J. Clin. Invest.* **118**, 2386–2389 (2008).
24. M. Ludlow, I. Allen, J. Schneider-Schaulies, Systemic spread of measles virus: Overcoming the epithelial and endothelial barriers. *Thromb. Haemost.* **102**, 1050–1056 (2009).

25. B. K. Rima, W. P. Duprex, New concepts in measles virus replication: Getting in and out in vivo and modulating the host cell environment. *Virus Res.* **162**, 47–62 (2011).
26. B. Crimeen-Irwin *et al*., Ligand binding determines whether CD46 is internalized by clathrin-coated pits or macropinocytosis. *J. Biol. Chem.* **278**, 46927–46937 (2003).
27. O. Pernet, C. Pohl, M. Ainouze, H. Kweder, R. Buckland, Nipah virus entry can occur by macropinocytosis. *Virology* **395**, 298–311 (2009).
28. C. Frecha *et al*., Measles virus glycoprotein-pseudotyped lentiviral vector-mediated gene transfer into quiescent lymphocytes requires binding to both SLAM and CD46 entry receptors. *J. Virol.* **85**, 5975–5985 (2011).
29. R. S. van Binnendijk, R. W. van der Heijden, A. D. Osterhaus, Monkeys in measles research. *Curr. Top. Microbiol. Immunol.* **191**, 135–148 (1995).
30. P. G. Auwaerter *et al*., Measles virus infection in rhesus macaques: Altered immune responses and comparison of the virulence of six different virus strains. *J. Infect. Dis.* **180**, 950–958 (1999).
31. R. K. Rowe, S. L. Brody, A. Pekosz, Differentiated cultures of primary hamster tracheal airway epithelial cells. *In Vitro Cell. Dev. Biol. Anim.* **40**, 303–311 (2004).
32. C. M. Newby, R. K. Rowe, A. Pekosz, Influenza A virus infection of primary differentiated airway epithelial cell cultures derived from Syrian golden hamsters. *Virology* **354**, 80–90 (2006).
33. R. K. Rowe, A. Pekosz, Bidirectional virus secretion and nonciliated cell tropism following Andes virus infection of primary airway epithelial cell cultures. *J. Virol.* **80**, 1087–1097 (2006).
34. C. D. Richardson, A. Scheid, P. W. Choppin, Specific inhibition of paramyxovirus and myxovirus replication by oligopeptides with amino acid sequences similar to those at the N-termini of the F1 or HA2 viral polypeptides. *Virology* **105**, 205–222 (1980).
35. M. Tahara *et al*., Measles virus infects both polarized epithelial and immune cells by using distinctive receptor-binding sites on its hemagglutinin. *J. Virol.* **82**, 4630–4637 (2008).
36. K. Takeuchi, N. Miyajima, N. Nagata, M. Takeda, M. Tashiro, Wild-type measles virus induces large syncytium formation in primary human small airway epithelial cells by a SLAM(CD150)-independent mechanism. *Virus Res.* **94**, 11–16 (2003).
37. J. Mercer, A. Helenius, Virus entry by macropinocytosis. *Nat. Cell Biol.* **11**, 510–520 (2009).
38. G. Torriani *et al*., Macropinocytosis contributes to hantavirus entry into human airway epithelial cells. *Virology* **531**, 57–68 (2019).
39. J. S. Rossman, G. P. Leser, R. A. Lamb, Filamentous influenza virus enters cells via macropinocytosis. *J. Virol.* **86**, 10950–10960 (2012).
40. S. Delpeut, G. Sisson, K. M. Black, C. D. Richardson, Measles virus enters breast and colon cancer cell lines through a PVRL4-mediated macropinocytosis pathway. *J. Virol.* **91**, e02191-16 (2017).
41. M. Essaidi-Laziosi *et al*., Propagation of respiratory viruses in human airway epithelia reveals persistent virus-specific signatures. *J. Allergy Clin. Immunol.* **141**, 2074–2084 (2018).
42. L. Zhang, P. L. Collins, R. A. Lamb, R. J. Pickles, Comparison of differing cytopathic effects in human airway epithelium of parainfluenza virus 5 (W3A), parainfluenza virus type 3, and respiratory syncytial virus. *Virology* **421**, 67–77 (2011).
43. N. H. Wu *et al*., The differentiated airway epithelium infected by influenza viruses maintains the barrier function despite a dramatic loss of ciliated cells. *Sci. Rep.* **6**, 39668 (2016).
44. R. Villenave *et al*., In vitro modeling of respiratory syncytial virus infection of pediatric bronchial epithelium, the primary target of infection in vivo. *Proc. Natl. Acad. Sci. U.S.A.* **109**, 5040–5045 (2012).
45. M. Porotto *et al*., Authentic modeling of human respiratory virus infection in human pluripotent stem cell-derived lung organoids. *mBio* **10**, e00723-19 (2019).
46. L. Zhang, M. E. Peeples, R. C. Boucher, P. L. Collins, R. J. Pickles, Respiratory syncytial virus infection of human airway epithelial cells is polarized, specific to ciliated cells, and without obvious cytopathology. *J. Virol.* **76**, 5654–5666 (2002).
47. R. M. Liesman *et al*., RSV-encoded NS2 promotes epithelial cell shedding and distal airway obstruction. *J. Clin. Invest.* **124**, 2219–2233 (2014).
48. L. Zhang *et al*., Infection of ciliated cells by human parainfluenza virus type 3 in an in vitro model of human airway epithelium. *J. Virol.* **79**, 1113–1124 (2005).
49. J. Rosenblatt, M. C. Raff, L. P. Cramer, An epithelial cell destined for apoptosis signals its neighbors to extrude it by an actin- and myosin-dependent mechanism. *Curr. Biol.* **11**, 1847–1857 (2001).
50. S. A. Gudipaty, J. Rosenblatt, Epithelial cell extrusion: Pathways and pathologies. *Semin. Cell Dev. Biol.* **67**, 132–140 (2017).
51. Y. Gu, T. Forostyan, R. Sabbadini, J. Rosenblatt, Epithelial cell extrusion requires the sphingosine-1-phosphate receptor 2 pathway. *J. Cell Biol.* **193**, 667–676 (2011).
52. G. T. Eisenhoffer *et al*., Crowding induces live cell extrusion to maintain homeostatic cell numbers in epithelia. *Nature* **484**, 546–549 (2012).
53. M. A. Mulvey *et al*., Induction and evasion of host defenses by type 1-piliated uropathogenic Escherichia coli. *Science* **282**, 1494–1497 (1998).
54. P. Muenzner, V. Bachmann, W. Zimmermann, J. Hentschel, C. R. Hauck, Human-restricted bacterial pathogens block shedding of epithelial cells by stimulating integrin activation. *Science* **329**, 1197–1201 (2010).
55. M. A. Mulvey, J. D. Schilling, J. J. Martinez, S. J. Hultgren, Bad bugs and beleaguered bladders: Interplay between uropathogenic Escherichia coli and innate host defenses. *Proc. Natl. Acad. Sci. U.S.A.* **97**, 8829–8835 (2000).
56. M. Kim *et al*., Bacteria hijack integrin-linked kinase to stabilize focal adhesions and block cell detachment. *Nature* **459**, 578–582 (2009).
57. N. Tegtmeyer, S. Backert, Bacterial type III effectors inhibit cell lifting by targeting integrin-linked kinase. *Cell Host Microbe* **5**, 514–516 (2009).
58. S. M. Frisch, H. Francis, Disruption of epithelial cell-matrix interactions induces apoptosis. *J. Cell Biol.* **124**, 619–626 (1994).
59. K. Bertrand, Survival of exfoliated epithelial cells: A delicate balance between anoikis and apoptosis. *J. Biomed. Biotechnol.* **2011**, 534139 (2011).
60. C. Fung, R. Lock, S. Gao, E. Salas, J. Debnath, Induction of autophagy during extracellular matrix detachment promotes cell survival. *Mol. Biol. Cell* **19**, 797–806 (2008).
61. R. Lock, J. Debnath, Extracellular matrix regulation of autophagy. *Curr. Opin. Cell Biol.* **20**, 583–588 (2008).
62. P. G. Holt, D. H. Strickland, M. E. Wikström, F. L. Jahnsen, Regulation of immunological homeostasis in the respiratory tract. *Nat. Rev. Immunol.* **8**, 142–152 (2008).
63. A. C. Kirby, M. C. Coles, P. M. Kaye, Alveolar macrophages transport pathogens to lung draining lymph nodes. *J. Immunol.* **183**, 1983–1989 (2009).
64. F. Herschke *et al*., Cell-cell fusion induced by measles virus amplifies the type I interferon response. *J. Virol.* **81**, 12859–12871 (2007).
65. I. Fugier-Vivier *et al*., Measles virus suppresses cell-mediated immunity by interfering with the survival and functions of dendritic and T cells. *J. Exp. Med.* **186**, 813–823 (1997).
66. B. K. Singh *et al*., The nectin-4/afadin protein complex and intercellular membrane pores contribute to rapid spread of measles virus in primary human airway epithelia. *J. Virol.* **89**, 7089–7096 (2015).
67. B. K. Singh, C. K. Pfaller, R. Cattaneo, P. L. Sinn, Measles virus ribonucleoprotein complexes rapidly spread across well-differentiated primary human airway epithelial cells along F-actin rings. *mBio* **10**, e02434-19 (2019).
68. B. György *et al*., Membrane vesicles, current state-of-the-art: Emerging role of extracellular vesicles. *Cell. Mol. Life Sci.* **68**, 2667–2688 (2011).
69. D. G. Meckes Jr, N. Raab-Traub, Microvesicles and viral infection. *J. Virol.* **85**, 12844–12854 (2011).
70. J. M. Silverman, N. E. Reiner, Exosomes and other microvesicles in infection biology: Organelles with unanticipated phenotypes. *Cell. Microbiol.* **13**, 1–9 (2011).
71. W. J. Moss, D. E. Griffin, Measles. *Lancet* **379**, 153–164 (2012).
72. N. Ono *et al*., Measles viruses on throat swabs from measles patients use signaling lymphocytic activation molecule (CDw150) but not CD46 as a cellular receptor. *J. Virol.* **75**, 4399–4401 (2001).